

Fitting a self-consistent physical model to the power spectral density of XTE J1550-564

Adam Ingram*

Durham University

E-mail: a.r.ingram@durham.ac.uk

Chris Done

Durham University

The variability properties of Black Hole Binaries (BHBs) have been studied for well over 20 years and a very detailed phenomenological picture has been developed, particularly of the properties of the Power Spectral Density (PSD). However, the underlying physical processes that generate the variability are very poorly understood, especially low frequency Quasi Periodic Oscillations (QPOs). We describe a model that associates the QPO with Lense-Thirring Precession of the hot inner flow and show how this process is affected by fluctuations in mass accretion rate which themselves generate broadband variability power. This causal connection between physical processes allows us to define a full, self-consistent model of the PSD which we fit to data from the 1998 outburst of XTE J1550-564. This is the first ever attempt to fit a physical model of the PSD to data.

Fast X-ray timing and spectroscopy at extreme count rates

February 7-11, 2011

Champéry, Switzerland

*Speaker.

1. Introduction

Emission observed from Black Hole Binaries (BHBs) is variable on a broad range of timescales. On the longest timescales (\sim weeks), these sources are seen to transition between quiescence, when they are hardly visible above the X-ray background; and outburst, when they are amongst the brightest X-ray objects in the sky. During the rise from quiescence to outburst, the source always displays an evolution in spectral state. At the lowest luminosities, the source is observed to be in the low/hard state, with the Spectral Energy Distribution (SED) dominated by a hard (photon index $\Gamma < 2$) power law tail but also including a weak disc component and reflection features. The disc is then seen to increase in luminosity (and average mass accretion rate, \dot{M}_0) as the power law softens ($\Gamma \sim 2$) and the reflection fraction increases (intermediate state). As the luminosity increases further, the SED either becomes almost completely disc dominated (high/soft state) or it displays both a strong disc component with a soft ($\Gamma > 2$) power law tail (very high state; see review by Done, Gierliński & Kubota 2007).

The SED of the low/hard state can be explained by a two component model whereby the standard cool, optically thick, geometrically thin accretion disc (Shakura & Sunyaev 1973) is truncated at some radius r_o which is greater than the last stable orbit, r_{lso} . Interior to this is a hot, optically thin, geometrically thick accretion flow, perhaps similar to an Advection Dominated Accretion Flow (ADAF; Narayan & Yi 1995). We observe a fraction of the disc emission directly but some of the photons emitted by the disc are incident upon the flow where they are Compton up scattered by the hot electrons thus creating the power law tail. As the source evolves, the truncation radius decreases which increases both the amount of direct disc emission and the number of seed photons incident on the flow thus softening the power law index of the flow emission. It is therefore possible to describe the spectral evolution throughout the rise to outburst by assuming r_o to decrease as the average mass accretion rate increases until $r_o \approx r_{lso}$ in the high/soft state. Although this is the model we consider, it is important to note that alternative geometries are suggested in the literature (e.g. Miller, Homan & Miniutti 2006) and the position of the disc inner radius is still an open issue.

Further complexity can be revealed by appreciating that the spectral shapes discussed so far are actually averaged over $\sim 2000s$. During this time interval the normalisation *and* shape of the SED fluctuate on timescales as short as $\sim 0.1s$ (Sobolewska & Zycki 2005). A power spectral analysis of the total luminosity reveals Quasi-Periodic Oscillations (QPOs) superimposed on a broad band noise of variability. The broad band noise can be described using broad Lorentzians centred at characteristic frequencies f_b and f_h , often referred to as the low and high break frequencies. The QPO harmonics can be described by narrow Lorentzians centred at f_{QPO} , $2f_{QPO}$ etc (e.g. Belloni, Psaltis & van der Klis 2002). As the SED evolves, so does the power spectral density (PSD). The characteristic frequencies f_b , f_h and f_{QPO} are seen to increase with luminosity and are in fact correlated (Wijnands & van der Klis 1999; Klein-Wolt & van der Klis 2008; van der Klis 2004; Psaltis, Belloni & van der Klis 1999). The high frequency ($> 10 Hz$) tail in the PSD, however, remains constant despite the increase in f_b , f_h and f_{QPO} (Gierliński, Nikołaćuk, & Czerny 2008). Although the variability properties have been studied for over 20 years, the underlying physical processes are still poorly understood.

There are many proposed QPO mechanisms in the literature, some of which are based on a misalignment between the angular momentum of the black hole and that of the binary system (e.g.

Stella & Vietri 1998; Ingram, Done & Fragile 2009, hereafter IDF09) and others are associated with wave modes in the accretion flow (e.g. Cabanac et al 2010). In IDF09, we outlined a QPO model based on the relativistic precession model of Stella & Vietri (1998) whereby the QPO frequency is given by the Lense-Thirring precession frequency at the truncation radius. Lense-Thirring precession is a relativistic effect which occurs because of the asymmetric gravitational potential present around a spinning black hole. If a test mass approaches the black hole on a trajectory not orthogonal to the black hole angular momentum vector, its orbit will precess because spacetime is being dragged around the black hole so as the particle reaches the starting point of its orbit (i.e. $\phi = 0, 2\pi, etc$), that point in spacetime has actually rotated some way around the black hole. In BHs, we may expect the plane of the binary orbit to be misaligned with that of the black hole spin and therefore this effect should be present. Fragile et al (2007; 2009) run General Relativistic Magnetohydrodynamic (GRMHD) simulations of a misaligned large scale height accretion flow, predicted to be present near the black hole by the truncated disc model, and show that it can precess as a solid body. This is possible because warps in such a flow are communicated by bending waves so the characteristic communication timescale is the sound crossing time which is *shorter* than the precession period. In IDF09, we found that a configuration whereby the disc is stationary but the flow is precessing can predict a QPO frequency very close to that observed for $50 > r_o > 10$ as is implied by the SED evolution. This model is also attractive because it ties the QPO to the hot flow which is required by the data (Sobolewska & Zycki 2005).

The underlying viscosity mechanism in the flow is most likely the Magneto Rotational Instability (MRI). It is looking increasingly likely that this is also the underlying source of broad band variability in the flow as it seems to generate large fluctuations in all quantities (e.g. Krolik & Hawley 2002). The temporal variability generated by the MRI extends to very high frequencies but the emission is inherently linked to the reservoir of available gravitational energy and therefore should depend on the mass accretion rate \dot{M} . It is commonly assumed that the variability in \dot{M} at a given radius is characterised by the local viscous frequency, $f_{visc}(r)$, where $f_{visc}(r) \propto r^{-3/2}$ in the simplest case. This interpretation implies that $f_b \approx f_{visc}(r_o)$ and $f_h \approx f_{visc}(r_i)$ where r_i is the inner radius of the flow (e.g. Ingram & Done 2010). Although this is a rather crude approximation, it is a very attractive toy model because the low frequency noise is tied to the truncation radius but the high frequency noise is not meaning that the observed evolution of both the PSD and SED can be naturally explained with a moving truncation radius.

Another fundamental property of the data which must be reproduced by any variability model is the sigma-flux relation (Uttley & McHardy 2001). This can be measured by splitting the light curve into $\sim 3s$ segments and finding the average and standard deviation of each segment. After binning, the standard deviation is always seen to be linearly related to the average flux. This tells us that the variability must be correlated across all timescales and therefore, in a picture where different temporal frequencies come predominantly from different spacial regions, there must be a causal connection between those regions. So a simple shot noise model with variability being generated locally in \dot{M} cannot reproduce the observations but the sigma-flux relation *can* be reproduced if the fluctuations in \dot{M} generated at a given radius *propagate* inward towards the black hole as might be intuitively expected (Lyubarskii 1997; Arevalo & Uttley 2006 hereafter AU06, Kotov et al 2001).

2. The Model

2.1 Propagating mass accretion rate fluctuations

The model reproduces the broad band noise with propagating mass accretion fluctuations (Lyubarskii 1997; Kotov et al 2001; AU06). We mainly follow the method of AU06 with a few differences. First, we split the flow up into N annuli with equal logarithmic spacing such that dr_n/r_n is constant. The MRI produces variability up to very high frequencies but the response of the flow should damp mass accretion rate fluctuations at frequencies higher than the local viscous frequency, $f_{visc}(r_n)$. For this reason, we assume that the power spectrum of fluctuations generated at the n^{th} annulus is given by a zero centred Lorentzian which cuts off at $f_{visc}(r_n)$. We can then use the method of Timmer & Koenig (1995) to generate the mass accretion rate fluctuations at each annulus, $\dot{m}(r_n, t)$.

We then must parameterise the viscous frequency. This is often assumed to be $f_{visc}(r) = \alpha(h/r)^2 f_k(r)$ where α is the viscosity parameter, h/r the flow semi-thickness and f_k the Keplerian frequency (Shakura & Sunyaev 1973). However, this is essentially a prescription rather than a prediction. Both Simulations (e.g. Fragile et al 2007) and analytical calculations for ADAFs (e.g. Gammie & Popham 1998) predict a steeper r dependence for f_{visc} than the Shakura Sunyaev prescription. For this reason, we parameterise the viscous frequency as $f_{visc}(r) = Br^{-m} f_k(r)$ and leave B and m as free parameters. Here (and hereafter), r is expressed in units of $R_g = GM/c^2$. In this prescription, the infall velocity, $v_r(r)$ is given by $v_r(r) = -f_{visc}(r)rR_g$.

We normalise each of the $\dot{m}(r_n, t)$ functions to have an average of unity and a fractional variability $\sigma/I = F_{var}/\sqrt{N_{dec}}$ where F_{var} is the fractional variability per decade in radial extent and N_{dec} is the number of annuli per decade in radial extent. The mass accretion rate at the outermost annulus, in units of the average mass accretion rate \dot{M}_0 , is then given by $\dot{M}(r_1, t) = \dot{m}(r_1, t)$. This then propagates to the next annulus at a speed $v_r(r_1)$ over a distance dr_1 and therefore arrives after a time $t_{lag} = -R_g dr_1/v_r(r_1)$. The mass accretion rate at the next annulus is then given by $\dot{M}(r_2, t) = \dot{M}(r_1, t - t_{lag})\dot{m}(r_2, t)$ which, for the n^{th} annulus, generalises to $\dot{M}(r_n, t) = \dot{M}(r_{n-1}, t - t_{lag})\dot{m}(r_n, t)$, where $t_{lag} = -R_g dr_n/v_r(r_n)$. At the N^{th} annulus, $r_N = r_i$ which is the inner radius of the flow.

In order to then create a light curve, we must assume an emissivity such that the luminosity (in units of $\dot{M}_0 c^2$) is given by $dL(r_n, t) = \eta/2 \dot{M}(r_n, t)\epsilon(r_n)r_n dr_n$ where $\epsilon(r_n) = \epsilon_0 r_n^{-\gamma} b(r_n)$, γ is the emissivity index, η the accretion efficiency, $b(r)$ the boundary condition and ϵ_0 is a normalisation constant. Gravitational energy in the flow goes as $\gamma = 3$ but this just sets the *total* energy in the reservoir. A different emissivity is fine as long as ϵ_0 is set such that the energy emitted is equal to $\eta/2$ times the amount of gravitational energy in the flow. In Ingram & Done (2011), we consider two boundary conditions: the ‘stress free’ boundary condition $b(r) = 3(1 - \sqrt{r_n/r_i})$ and the ‘stressed’ boundary condition $b(r) = 1$. Here however, we just look at the stressed case as this gives a better statistical fit to the data.

Figure 1 shows a 20s segment of a light curve (left) generated using this method next to its power spectrum. We assume a black hole mass of $10M_{sun}$ and a spin of $a_* = 0.5$. We assume $r_i = 2.5$, $r_o = 20$, $F_{var} = 0.4$, $B = 0.03$, $m = 0.5$, $\gamma = 4.5$ and $b(r) = 1$. We sum over $N = 30$ annuli and simulate a light curve with 2^{22} time steps, giving a duration of 4096s (similar to a typical RXTE observation) for a time bin of $dt = 9.7 \times 10^{-4}$. The right hand plot of Figure 1 shows that the generated light curve has a linear sigma-flux relation in agreement with the data.

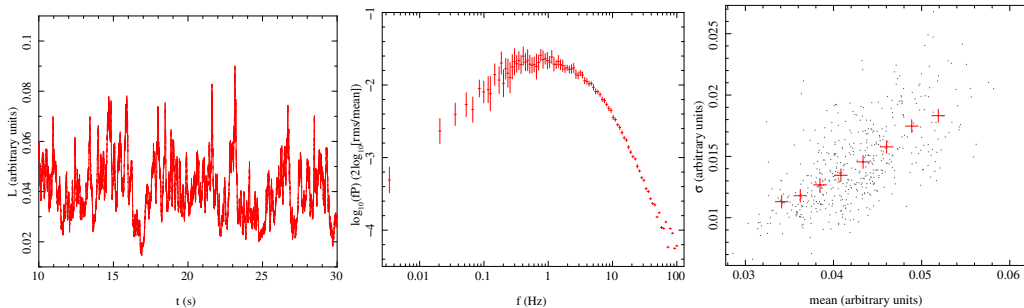


Figure 1: *Left:* A 20s segment of the simulated light curve. *Middle:* The power spectrum of the simulated light curve. *Right:* The sigma-flux relation for the simulated light curve which is linear as observed.

2.2 Lense-Thirring precession

In a geometry whereby a hot inner flow is precessing as a solid body (as shown in GRMHD simulations; e.g. Fragile et al 2007) interior to a stationary disc, the precession frequency should modulate the x-ray emission to give a QPO at the precession frequency. The precession frequency of the flow is given by

$$f_{prec} = f_{QPO} = \frac{\int_{r_i}^{r_o} f_{LT} \Sigma f_k r^3 dr}{\int_{r_i}^{r_o} \Sigma f_k r^3 dr} \quad (2.1)$$

(Liu & Melia 2002) where Σ is the surface density and

$$f_{LT} = f_k \left[1 - \sqrt{1 - \frac{4a_*}{r^{3/2}} + \frac{3a_*}{r^2}} \right] \quad (2.2)$$

is the point particle Lense-Thirring precession frequency. In the previous section, we calculated $\dot{M}(r_n, t)$ and assumed a form for $v_r(r_n)$, therefore we can easily calculate Σ merely by imposing mass conservation. In units of $\dot{M}_0/(cR_g)$, this gives $\Sigma(r_n, t) = -\dot{M}(r_n, t)/(2\pi r_n v_r(r_n))$ which reduces to $\Sigma(r_n, t) = \dot{M}(r_n, t)r^{m-1/2}/B$ in this case. This allows us to calculate the precession frequency without making *any* further assumptions! What is more, we see that it fluctuates which allows the model to produce a quasi periodic oscillation rather than a periodic one.

It is possible to calculate a light curve from this geometry and recover non-sinusoidal variability (i.e. harmonic structure). This calculation, however, is far from trivial and will be the subject of a future paper (Ingram, Done and Zycki in prep). For now, we simply take the average precession frequency (over 4096s) to be f_{QPO} and represent the QPO with Lorentzians centred at f_{QPO} , $2f_{QPO}$, $3f_{QPO}$ and $1/2f_{QPO}$, giving the 1st, 2nd, 3rd and sub harmonics respectively. The standard deviation of the precession frequency σ_{prec} also gives an estimate for the QPO width, however, frequency jitter is not the only process that gives a QPO width, therefore we can only predict a lower limit. For our fits, we leave the width as a free parameter but require all the harmonics to have the same quality factor $Q = f_{QPO}/\sigma_{QPO}$ as required by the data (e.g. Rao et al 2010). We also leave the normalisation of each harmonic as a free parameter.

We generate a QPO light curve using the method of Timmer & Koenig (1995) and add this to the light curve already generated. We then have a model for the entire power spectrum which we fit to data from the 1998 rise to outburst of XTE J1550-564 in the next section.

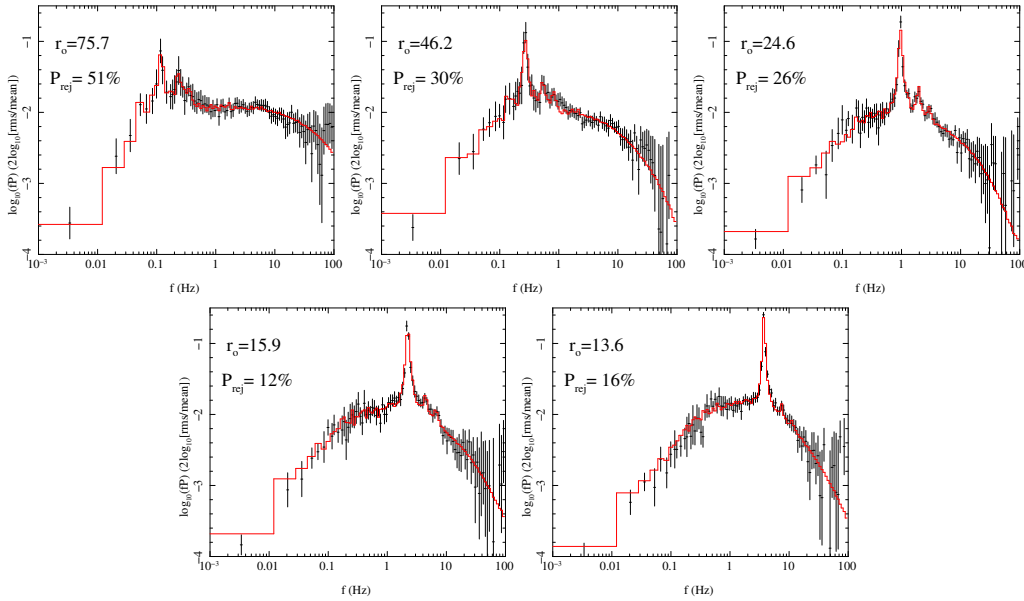


Figure 2: Fit results with $\gamma = 4.15$, $b(r) = 1$ and $r_i = 2.45$ for all 5 observations. The truncation radius, r_o , and rejection probability, P_{rej} , are included in the plots. Here, $m = 0.46 - 1.016$.

3. Fitting to XTE J1550-564

We are now ready to fit the model to data. We use RXTE data from the 1998 rise to outburst of XTE J1550-564 (Wilson & Done 2001; Rao et al 2010; Altamirano 2008). We look at 5 observations with the following observational IDs: 30188-06-03-00, 30188-06-01-00, 30188-06-01-03, 30188-06-05-00, 30188-06-11-00; hereafter observations 1-5 respectively. In order to avoid disc contamination, we only consider energy channels above 10 keV.

In order to get a good estimate of the power spectrum of both the observed and simulated light curves, we use logarithmically smoothed periodograms (Papadakis & Lawrence 1993). This involves splitting the light curve into M segments and calculating a periodogram for each, where the periodogram is given by the modulus squared of the discrete Fourier transform. The logarithmically smoothed periodogram is calculated by averaging over the logarithm of all of the periodograms.

We find our fit by minimising χ^2 but note that, because we are not dealing with strictly Gaussian errors, this may not be the most appropriate statistical test for goodness of fit. To make up for this, once we have minimised χ^2 for each of the 5 observations, we test the goodness of fit using the rejection probability method of Uttley et al (2002) and Markowiz et al (2003). This is a far more stringent statistical test than χ^2 which involves simulating > 500 light curves to create a distribution and then assessing the likelihood that the observed light curve does *not* belong to that distribution. A high rejection probability therefore constitutes a poor fit.

Figure 2 shows the resulting fits with the truncation radius and rejection probability displayed for each plot in the top left hand corner. They look like very good fits by eye and, indeed the rejection probabilities are low too. Here $r_i = 2.45$ and the power law index governing the viscous frequency $m = 0.46 - 1.016$. In a future paper (Ingram & Done in prep), we will explore the possibility that the viscous frequency is actually best represented by a smoothly broken power law

rather than a single power law with its index changing with time. If the index is ~ 0.5 above the break and ~ 1 below the break, it should be possible to fit these data simultaneously with the parameterisation of the viscous frequency held constant across the 5 observations. This will also give the same surface density profile as that predicted from GRMHD simulations (Fragile et al 2007; Ingram, Done & Fragile 2009).

4. Conclusions

We have developed a model whereby mass accretion rate fluctuations are generated in, and propagate through, a precessing flow. The mass accretion rate fluctuations give rise to the observed broad band variability and the propagation allows the model to reproduce a linear sigma-flux relation (Lyubarskii 1997; AU06; Uttley & McHardy 2001). It is then possible to constrain the precession frequency, which gives the QPO, using only mass conservation. It is therefore possible to self-consistently predict the shape of the broad band noise *and* the QPO frequency from one set of parameters which allows us to fit the first ever physically motivated model to the power spectrum of a BHB (Figure 2).

This model naturally predicts many of the observed correlations in the data. It reproduces the observed correlation between QPO and break frequency (Wijnands & van der Klis 1999) because both are dependent on the moving truncation radius, r_o . Also, the coherence of the QPO (characterised by the quality factor $Q = f_{QPO}/\sigma_{QPO}$) evolves with frequency. Q is seen to increase with frequency for $f_{QPO} < 0.2$ Hz after which, it generally remains constant for the rest of the transition (Rao et al 2010). The model predicts Q to rise with f_{QPO} because the variability in QPO frequency (which gives a lower limit for σ_{QPO}) is dependent on the total variability in mass accretion rate across the flow. Because the variability per decade in radial extent is constant, the total variability across the flow decreases with r_o giving a higher Q value. The model also predicts a linear relation between f_{QPO} and luminosity on short timescales ($\sim 3s$). This is because a perturbation (increase) in mass accretion rate at large r slows down precession but has little effect on the luminosity due to the emissivity weighting. When this perturbation has propagated to small r , it now speeds up precession and increases luminosity. This property has recently been observed in the same data set we fit our model to (Heil, Vaughan & Uttley 2011; Rao et al 2010).

The next step is to include an energy dependence and calculate the QPO light curve directly from a modulation mechanism rather than using Lorentzians as we have done here. This should allow the model to reproduce many more observations such as the frequency dependent time lags between energy bands (Nowak et al 1999) and the frequency resolved spectrum (Revnivtsev et al 1999). It is also very important to include disc variability (Wilkinson & Uttley 2009; also see Phil Uttley's contribution to this volume) and to properly take account of all general relativistic effects. With these improvements, this model has the potential to be powerfully predictive.

References

- [1] Altamirano D., 2008, PhDT,
- [2] Arévalo P., Uttley P., 2006, MNRAS, 367, 801
- [3] Belloni T., Psaltis D., van der Klis M., 2002, ApJ, 572, 392

- [4] Cabanac R. A., Valls-Gabaud D., Lidman C., 2008, MNRAS, 386, 2065
- [5] Done C., Gierliński M., Kubota A., 2007, A&ARv, 15, 1
- [6] Fragile P. C., Blaes O. M., Anninos P., Salmonson J. D., 2007, ApJ, 668, 417
- [7] Fragile P. C., Meier D. L., 2009, ApJ, 693, 771
- [8] Gammie C. F., Popham R., 1998, ApJ, 498, 313
- [9] Gierliński M., Nikolajuk M., Czerny B., 2008, MNRAS, 383, 741
- [10] Heil L. M., Vaughan S., Uttley P., 2010, arXiv, arXiv:1011.6321
- [11] Ingram A., Done C., Fragile P. C., 2009, MNRAS, 397, L101
- [12] Ingram A., Done C., 2010, MNRAS, 405, 2447
- [13] Ingram A., Done C., 2011, arXiv, arXiv:1101.2336
- [14] Klein-Wolt M., van der Klis M., 2008, ApJ, 675, 1407
- [15] Kotov O., Churazov E., Gilfanov M., 2001, MNRAS, 327, 799
- [16] Krolik J. H., Hawley J. F., 2002, ApJ, 573, 754
- [17] Liu S., Melia F., 2002, ApJ, 573, L23
- [18] Lyubarskii Y. E., 1997, MNRAS, 292, 679
- [19] Markowitz A., et al., 2003, ApJ, 593, 96
- [20] Miller J. M., Homan J., Miniutti G., 2006, ApJ, 652, L113
- [21] Narayan R., Yi I., 1995, ApJ, 452, 710
- [22] Nowak M. A., Vaughan B. A., Wilms J., Dove J. B., Begelman M. C., 1999, ApJ, 510, 874
- [23] Papadakis I. E., Lawrence A., 1993, MNRAS, 261, 612
- [24] Psaltis D., Belloni T., van der Klis M., 1999, ApJ, 520, 262
- [25] Rao F., Belloni T., Stella L., Zhang S. N., Li T., 2010, ApJ, 714, 1065
- [26] Revnivtsev M., Gilfanov M., Churazov E., 1999, A&A, 347, L23
- [27] Shakura N. I., Sunyaev R. A., 1973, A&A, 24, 337
- [28] Sobolewska M. A., Życki P. T., 2006, MNRAS, 370, 405
- [29] Stella L., Vietri M., 1998, ApJ, 492, L59
- [30] Timmer J., Koenig M., 1995, A&A, 300, 707
- [31] Uttley P., McHardy I. M., 2001, MNRAS, 323, L26
- [32] Uttley P., McHardy I. M., Papadakis I. E., 2002, MNRAS, 332, 231
- [33] van der Klis M., 2004, AdSpR, 34, 2646
- [34] Wijnands R., van der Klis M., 1999, ApJ, 514, 939
- [35] Wilkinson T., Uttley P., 2009, MNRAS, 397, 666
- [36] Wilson C. D., Done C., 2001, MNRAS, 325, 167